Model of ASCA X-ray spectrum of Kepler's SNR

Kenzo Kinugasa

Gunma Astronomical Observatory, 1-18-7, Ohtomo-machi, Maebashi, Gunma 371-0847, Japan

Hiroshi Tsunemi

Depertment of Earth and Space Science, Osaka University, 1-1 Machikaneyama-cho, Toyonaka, Osaka 560-0043, Japan

CREST, Japan Science and Technology Corporation (JST)

Anne Decourchelle

Service d'Astrophysique DAPNIA/DSM, CE-Saclay, F-91191 Gif-sur-Yvette Cedex, France

ABSTRACT

We report the results of Kepler's supernova remnant (SNR) observed with ASCA. We obtained the X-ray spectrum of Kepler's SNR in the energy range between 0.5 keV and 10 keV, clearly detected many emission lines from the heavy elements. The spectrum was not reproduced by a single temperature CIE and NEI model. Therefore, we constructed a realistic spectral model considering the SNR evolution; the Sedov and the Chevalier model. The X-ray spectrum of Kepler's SNR was not reproduced by the Sedov model, but well by the Chevalier model, except the Fe-K line blends. The emission from the ejecta heated by the reverse shock dominates that from the ISM heated by the blast wave. Kepler's SNR is not in the Sedov phase, but in the free-expansion phase. The abundance of the ejecta strongly suggests that Kepler's SN is a SN Ia. However, since the Fe-K line blends could not be reproduced well, another component producing the Fe-K line blends is needed. The Fe-K line emission is well produced by the additional iron component. This component must have a relatively higher temperature and a lower ionization timescale than these of the main ejecta. The iron component may be associated with the recently shocked material, probably the iron rich ejecta of SN Ia.

1. Introduction

Kepler's SNR is associated with one of the historical supernovae (SNe); its age is about 390 years. The distance, estimated by various ways, scatters in the range of 3 – 5 kpc. The position is $(\alpha, \delta)(\mathrm{J2000}) = (17^{\mathrm{h}}30^{\mathrm{m}}40\overset{\mathrm{s}}{.}8, -21^{\circ}29'20'')$, $(l, b) = (4\overset{\circ}{.}5, 6\overset{\circ}{.}8)$. Since Kepler's SNR is at a high galactic latitude, the height from the galactic plane is 360 – 600 pc. Kepler's SNR was observed from radio to X-ray wavelength.

Kepler's SN had been classified as a Type I SN (SN I) from the study of the historical light curve (Baade 1943). However, since its light curve was also shown to be consistent with a SN

II-L (Dogett, Branch 1985), the origin of Kepler's SNR has been a question for years. Its location seems to be more consistent with a SN Ia than a SN II, because the massive star is expected to be confined to the galactic plane. Also Kepler's SNR is one of the "Balmer-dominated" SNRs, like Tycho's SNR and SN 1006. Non detection of the point source like a pulsar so far, is consistent with SN Ia. On the other hand, the density of the ambient matter derived from X-ray observations is higher (1 cm^{-3} or more) (e.g., White, Long 1983; Hughes, Helfand 1985) than that expected from the height above the galactic plane (about 0.06 cm^{-3} expected from Lockman 1984). Slow moving knots were detected at the optical observation, suggesting the mass-loss by the progenitor (which must have been massive). The measurement of the chemical composition and the mass of the ejecta are important clues to determine the SN type of Kepler's SNR.

We present here the X-ray spectrum in the wide energy range of 0.5–10 keV with good energy resolution obtained with ASCA. We report the results of the spectrum fitting by the multi-temperature model based on the SNR model showing the metal abundance of the plasma. We discussed the SN type of Kepler's SN from the metal abundances. In this paper, we assume the distance to Kepler's SNR to be roughly 5 kpc (e.g., Hughes, Helfand 1985), we denote the source distance by D_5 normalized by 5 kpc.

2. Observations and Results

2.1. X-ray Spectrum

We observed Kepler's SNR on October 5 and 8, 1993 as a part of the performance verification phase programs. The data reported in this paper were obtained with two SISs. After the data reduction procedures, the total effective exposure time of the data used for spectrum analysis is about 23 ks both for SISs.

Figure 1 shows the X-ray spectrum in the energy range of 0.5–10 keV. We can clearly see many emission lines which can be easily identified from their energies. As the results of fitting with a powerlaw plus gaussians function, these lines are identified as $\mathrm{Mg}_{XI}\mathrm{K}\alpha$, $\mathrm{Mg}_{XI}\mathrm{K}\beta$, $\mathrm{Si}_{XIII}\mathrm{K}\alpha$, $\mathrm{Si}_{XIV}\mathrm{K}\alpha$, $\mathrm{Si}_{XIII}\mathrm{K}\beta$, $\mathrm{S}_{XV}\mathrm{K}\alpha$, $\mathrm{S}_{XVI}\mathrm{K}\beta$, $\mathrm{Ar}_{XVII}\mathrm{K}\alpha$, $\mathrm{Ca}_{XIX}\mathrm{K}\alpha$, and Fe-K line blends. We also notice that the continuum spectrum extends up to 10 keV region, which seems to be a common feature in young SNRs (e.g., Holt et al. 1994; Hwang et al. 1998). The center energy of the Fe-K line blends was 6.459 ± 0.013, which tells that the plasma does not reach the CIE condition. Moreover, the spectrum was not reproduced by a single temperature CIE nor NEI model.

2.2. SNR models and fittings

In order to understand the plasma components in Kepler's SNR, we introduced a multi-component model with a temperature gradient in the SNRs. We calculated the spectra of more

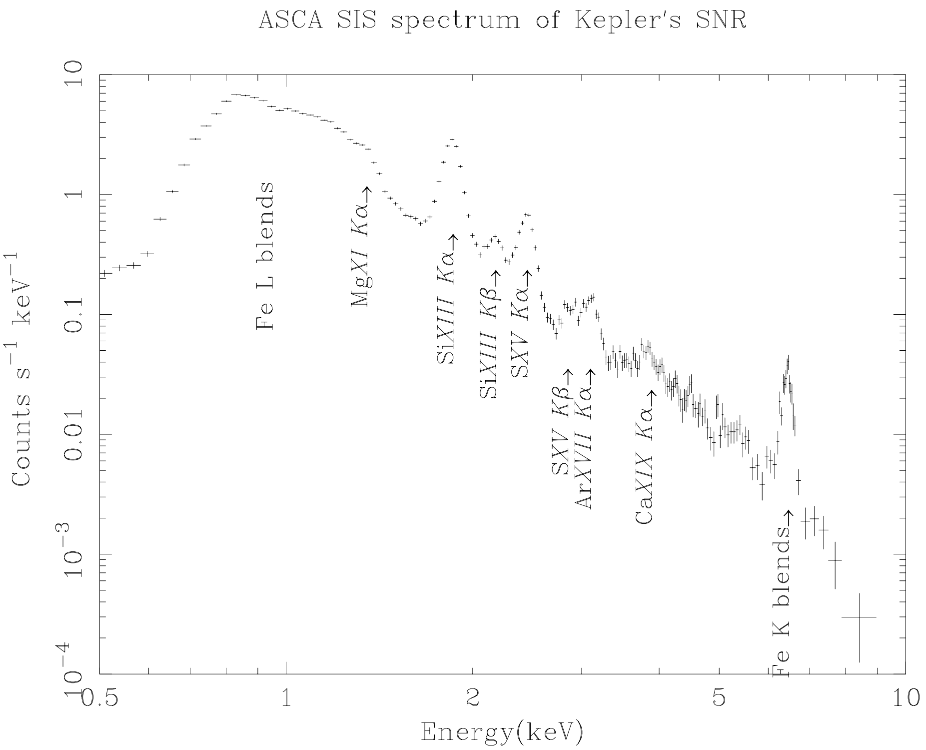

Fig. 1.— The X-ray spectrum of Kepler's SNR in the range of 0.5–10 keV obtained with SIS.

realistic models taking into account the model structure of SNRs. Since we focus on the X-ray characteristics and not upon hydrodynamic modeling, we will make use of existing hydrodynamic models, the Sedov model (Sedov 1959) for the adiabatic phase SNRs and the Chevalier model (Chevalier 1982) for the free-expansion phase SNRs.

At first, we tried to fit the data by the Sedov model. We left the metal abundance to be free in this model fitting. The best-fit spectrum are given in figure 2 (left). We found that the Sedov model could reproduce neither the high energy continuum nor the line emissions at low energy.

Next, we applied the Chevalier model to the data. We left the metal abundances of the ejecta to be free while those of the ISM is set to the solar value. Figure 2 (right) show the best-fit spectrum of the Chevalier model. We found that the Chevalier model could reproduce both the high energy continuum and the line center energy of the iron K line blends. However, we found that this model could not reproduce the intensity ratio between the Fe-K line blends and the Fe-L line blends.

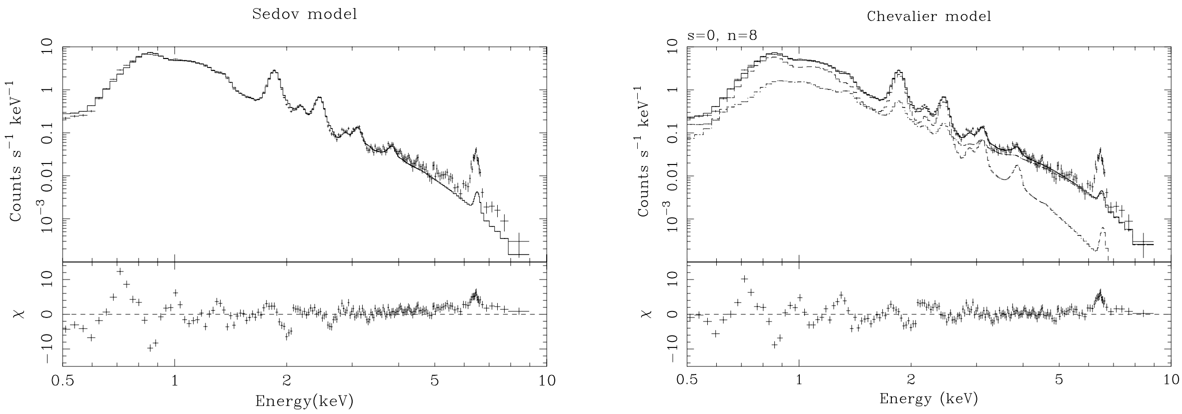

Fig. 2.— The best-fit spectra by the Sedov model (left) and the Chevalier model (right).

3. Discussions

As the results of the spectral analyses, the Chevalier model could reproduce the data better than the Sedov model. This fact shows that Kepler's SNR is not in the adiabatic phase, but in the free-expansion phase in which the emission from the reverse shock dominates that from the fore shock. Therefore, we can expect that the abundance we obtained shows the information of the ejecta.

It should be noted that the fitting results we obtained are based on the assumption that the abundances of He, C, and N are the solar values. However, this assumption may be inappropriate in Kepler's SNR. Since these elements only contribute to the continuum spectrum in the energy range we concerned, the relative abundances are more reliable than the absolute values which are derived from the model fitting. Therefore, in order to avoid the confusion due to this assumption, we consider the relative abundances normalized by that of Si. From figure 3, the abundances of the lighter elements (O, Ne, and Mg) are relatively low, and those of the heavier elements (S, Ar, and Ca) are high. Although the relative values of the iron and nickel abundances are still insufficient, this trend strongly favors the metal abundances of the nucleosynthesis expected from the SN Ia model rather than that from the SN II model. Detailed discussion on the deficiency of the iron and the Fe-K line blends is below.

We introduced another thermal component from the iron in order to reproduce the Fe-K line blends like that in Tycho's SNR (Hwang et al. 1998). We tried to fit the data by the best-fit Chevalier model along with an additional NEI component. Then we consider that the additional component can be considered to be made of iron. From the fitting results (figure 4), we found that the temperature of the additional iron component was $kT_e \sim 3$ keV, which is higher than the mean temperature of the reverse shock component. Whereas, the ionization time scale of this

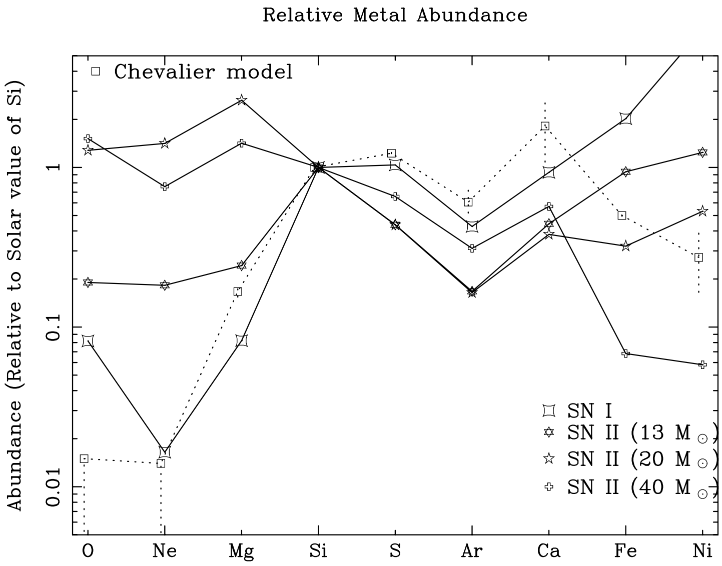

Fig. 3.— Relative abundance of the ejecta and the SN nucleosynthesis models (SN Ia and SN II). These values are normalized by Si.

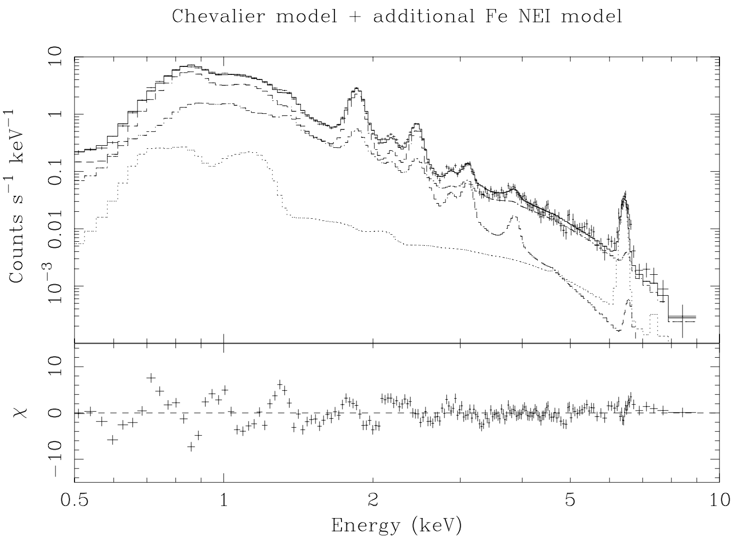

Fig. 4.— The data and the fitting model curve of the Chevalier model and an additional iron NEI model are shown. The each dot curve is the reverse shock component and the blast wave component of the Chevalier model, and the additional iron component.

component is $\log\tau \sim 9.5$, which is about one order lower. From the normalization and the iron abundance of the iron component, we roughly estimate the iron mass to be

$$M_{\rm Fe} \sim 0.4 \left(\frac{f}{0.25}\right)^{1/2} D_5^{5/2}\ {\rm M}_\odot, \qquad (1)$$

) where f is a filling factor. These values suggest that the iron component is more recently shocked than the Si, S, ejecta, which probably originate from the iron rich ejecta of SN Ia. Due to the insufficient spatial resolution of ASCA, we could not resolve where the iron component comes from. Future missions (AXAF, XMM, Astro-E, etc.) with a high spatial resolution imaging capability in the high energy band will enable us to resolve the stratification of the ejecta on Kepler's SNR.

REFERENCES

Baade W. 1943, ApJ, 97, 119

Chevalier R.A., 1982, ApJ, 258, 790

Doggett, J.B., and Branch, D. , AJ, 90, 2303

Holt S.S., Gotthelf E.V., Tsunemi H., Negoro H. 1994, PASJ, 46, L151

Hughes J.P., and Helfand D.J. 1985, ApJ, 291, 544

Hwang U., Hughes J.P., Petre R. 1998, ApJ, 497, 833

Lockman, F.J. 1984, ApJ, 283, 90

Sedov L.I. 1959, Similarity and Dimensional Methods in Mechanics (New York: Academic Press)

White R.L., and Long K.S. 1883, ApJ, 264, 196

This preprint was prepared with the AAS LaTeX macros v4.0.